Revista Facultad de Ingeniería No. 26. pp. 79-89. Junio, 2002

Theoretical model for heat transfer in the single crystal making

Farid Chejne[*], *Whady Flórez*[**], *Tamila Ragimova*[***] *and Juan P. Hernández*[**]

(Recibido el 15 de septiembre de 2001)

Abstract

A mathematical model has been developed that describes the heat transfer process during melt solidification and to define axial and radial thermal profile in both phases, solid and liquid. With this model we can obtain the geometric interface profile. Also we can study the influence of the main parameters such as the Biot number, the Peclet number and the lowering rate of the ampoule. We have used this model to give a conceptual explanation about heat transfer phenomena involved in another process like single crystal making.

---------- *Key words:* crystal making, crystal growth, heat transfer, furnaces.

Modelo teórico de la transferencia de calor en el crecimiento de monocristales

Resumen

Se ha desarrollado un modelo matemático que describe el proceso de transferencia de calor durante la solidificación y que define el perfil térmico axial y radial en ambas fases, sólida y líquida. Con este modelo podemos obtener el perfil geométrico de la interfaz.

También podemos estudiar la influencia de los principales parámetros como el número de Biot, el número de Peclet y la disminución de la tasa de la ampolla. Usamos este modelo para dar una explicación conceptual sobre los fenómenos de transferencia de calor incluidos en otros procesos como la fabricación de monocristales.

---------- *Palabras clave:* fabricación de cristales, crecimiento de cristales, solidificación, transferencia de calor, hornos.

* Grupo Recursos y Procesos Térmicos. Instituto de Energía. Escuela de Procesos y Energía. Universidad Nacional de Colombia. A.A. 1027, Medellín.

** Instituto de Energía y Termodinámica. Universidad Pontificia Bolivariana. A.A 56006, Medellín.

*** Universidad de Antioquia. A.A. 1226, Medellín, Colombia.

Introduction

The formation of the crystalline phase starting with the melting is called solidification process. This process is accompanied by a heat extraction and performs two stages: the initial crystal nucleation and the growth of these crystals by means of atom addition from the liquid phase. If only the formation of a unique nucleus were allowed in this process, an entire single crystal should be obtained. This is the main objective that is pursued in the single crystal making by the BRIDGMAN method.

A scheme of the furnace for single crystal making by means of the Bridgman method is shown in figure 1. The furnace owns a high temperature zone (T_H) and a low temperature one (T_C) and within both there is a zone where an axial temperature gradient is established.

The material to be processed is introduced into a cylindrical quartz ampoule with radius a. This ampoule is lowered down axially with constant velocity v through the temperature gradient of the furnace. The material is molten in the high temperature zone and is solidified in the low temperature one. The solidification begins at an intermediate point called interface.

The present work describes a mathematical method to obtain the radial and axial thermic profiles in homogeneous phases solidification process of semiconductors.

Papers that have given a numerical solution to the one-dimensional non-steady problem exist but they do not determine the morphology of the interface [1, 2, 3]. Other works have shown an analytic solution that displays the morphology of the interface [4, 5]. In the present work, an analytic two-dimensional steady solution is shown to provide information about the thermal profile both at the molten and the solid phases and which accounts for the morphology of the interface, outstanding conceptual aspects on heat transfer phenomena involved in the solidification process.

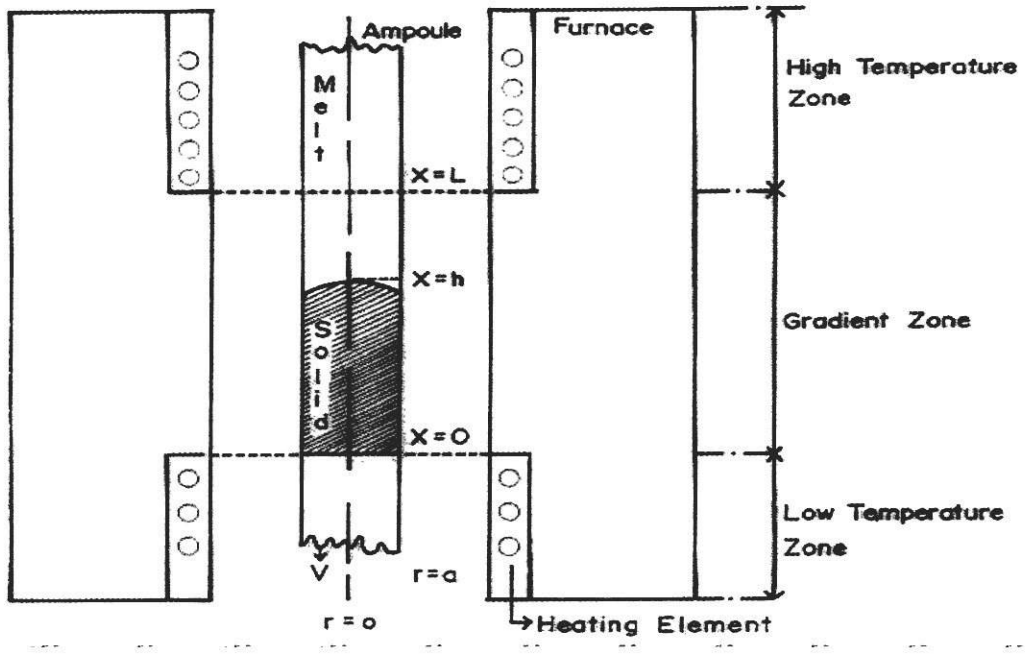

Figure 1 Scheme of the Bridgman furnace with the reference frames used in calculation

Solidification model

To propose this model the steady case (time independent) was considered. This allows to avoid the use of immobilisation variables in a reference frame attached to an infinite length ampoule moving vertically inside the furnace at a velocity v equal to the each layer formed velocity *R*. These two velocities are not equal in the transient case [1-6].

In this model, the reference frame that must be placed at the ampoule is the same that is attached to the furnace since the interface will be fixed at a position $x' = h$ (figure 1).

The equations defining the steady state process apply both for the solid phase and the melting and all have the form,

$$\frac{\partial^2 T_i}{dr^2} + \frac{1}{r}\frac{\partial T_i}{\partial r} + \frac{\partial^2 T_i}{\partial x^2} + \frac{V}{\alpha_i}\frac{\partial T_i}{\partial x'} = 0 \qquad (1)$$

where $i = S, L$ as it corresponds to the solid on the liquid phase. T_i is the temperature, r is the radial coordinate, x_i represents the axial distance. V and α are in their order, ampoule's lowering rate and thermal disfusivity.

By carrying out suitable changes on the variables (see table 1), expression (1) becomes,

$$\frac{\partial^2 \theta_i}{\partial \rho^2} + \frac{1}{\rho}\frac{\partial \theta_i}{\partial \rho} + \frac{\partial^2 \theta_i}{\partial x^2} + Pe_i \frac{\partial \theta_i}{\partial x} = 0 \qquad (2)$$

for $i = S, L$. θ, $\rho = r/a$ and $x = x'/a$, are the dimensionless variables that corresponds to T, r and x' respectively, and Pe is the Peclet number.

The boundary conditions of the problem are:

Table 1 Parameters used in the mathematical model

Parameter	*Value*
L	28,5 cm
a	0,95 cm
T_H	1.000 °C
T_C	750 °C
K_L	0,072 W/°K.cm
K_S	0,047 W/°K.cm
α_L	0,015 cm²/s
α_S	0,010 cm²/s
ΔH_f	148 J/gr
$\theta_{eq,S}$	0,8
$\theta_{eq,L}$	0,2

1. A symmetry condition at the center of the ampoule and an energy balance on the surface of the ampoule, which are respectively expressed as,

$$r = 0, \quad \rho = 0, \quad \frac{\partial \theta_i}{\partial \rho} = 0 \qquad (3)$$

$$r = a, \quad \rho = 1, \quad \frac{\partial \theta_i}{\partial \rho} = B_i(\theta_i - \theta_\infty) \qquad (4)$$

In above equations *Bi* is the Biot number, α is the ampoule radius and θ_∞ the temperature of the zone between the ampoule and furnace walls.

2. The axial thermal profile of the inner wall of the furnace at the zone of the gradient is,

$$T = (TH\text{-}TC)\frac{x'}{L} + TC \qquad (5)$$

The temperature difference between ends of gradient zone in the furnace is T_H - T_C and L is the length of the gradient zone.

3. The dimensionless temperature at the ends of the zone of the gradient (see *figure 1*) is,

$$x' = 0, \quad \theta_S = 0 \tag{6}$$

$$x' = L, \quad \theta_L = 0 \tag{7}$$

As consequence the spacial variable dimensionless is x = L/a

4. The energy balance at the interface is,

$$x' = h, \quad \theta_S = \theta_L = \theta_{eq} \tag{8}$$

$$-k_S \frac{\partial \theta_S}{\partial x'} = -k_L \frac{\partial \theta_L}{\partial x'} + \frac{Va\rho_L \Delta H}{T_H - T_C} \tag{9}$$

$$\theta_{eq} = \frac{T_f - T_C}{T_H - T_C} \tag{10}$$

The term θ_{eq} in equation (10) is the dimensionless fusion temperature and T_f is the fusion absolute temperature of semiconductor sample.

The solution of equation (2) is fulfilled by the variable separation method and we obtain,

$$\theta_S = \frac{T_S - T_L}{T_H - T_C} = \sum_{n=0}^{\infty} c_n J_0(\lambda_n \rho) \sinh(\lambda_n^* x) \tag{11}$$

$$\theta_L = \frac{T_H - T_L}{T_H - T_C} = \sum_{n=0}^{\infty} c'_n J_0(\lambda'_n \rho) \sinh(\lambda_n'^* x) \tag{12}$$

In equations (9) to (12), k_i is the thermal conductivity where $i=S$ or $i=L$ as it corresponds to the solid or liquid phase. V is the lowering rate of the ampoule and ΔH represents fusion enthalpy.

The eigenvalues λ and λ^* for solid phase and λ' and $\lambda^{*'}$ for liquid phase are calculated by means of the following equations:

$$\lambda^* = \sqrt{\left(\frac{P_e}{2}\right)^2 + \lambda^2} \tag{13}$$

The same structure is valid for λ' and λ^*.

$$\lambda_n J_1(\lambda_n) = B_i J_0(\lambda_n) - \frac{1}{c_n \lambda_n^* \cosh\left(\lambda_n^* \left(\frac{L}{a}\right)\right)} \tag{14}$$

$$\lambda_n' J_1(\lambda_n') = B_i J_0(\lambda_n') - \frac{1}{c_n' \lambda_n^{*'} \cosh\left(\lambda_n^{*'} \left(\frac{L}{a}\right)\right)} \tag{15}$$

Where $J_0(x)$ and $J_1(x)$ are in their order, bessel functions of zeroth and first order. The constants c_n and c_n' are found as follows,

$$c_n = \frac{\theta_{eq,L} \int_0^1 \rho J_0(\lambda_n \rho) d\rho}{senh(\lambda_n^*) \int_0^1 \rho J_0^2(\lambda_n \rho) d\rho} \tag{16}$$

$$c_n' = \frac{\theta_{eq,L} \int_0^1 \rho J_0(\lambda_n' \rho) d\rho}{senh(\lambda_n'^* (h/a - L/a)) \int_0^1 \rho J_0^2(\lambda_n' \rho) d\rho} \tag{17}$$

$$V = \frac{T_H - T_C}{a\Delta H}\left(k_S\theta_{eq,s}\coth\left(\lambda_n^*(h/a)\right)\right) -$$

$$k_L\theta_{eq,L}\coth\left[\lambda_n^*(h/a - L/a)\right] \qquad (18)$$

The configuration an position of the interface can be obtained from the relation (18), by the Newtonian method or some other analogous method to find the position of each point in the interface.

Numerical solution

This was gained by a program on FORTRAN and structured in a modular way.

The program has several procedures aiming at the calculation of Bessel functions by making use of the conventional power series expansion, that is,

$$J_n(x) = \sum_{m=0}^{\infty}\frac{(-1)^m}{m!(n+m)!}\left(\frac{x}{2}\right)^{n+2m} \qquad (19)$$

the convergence criterion used in this procedure fixes the exactness in the calculation of $J_n(x)$ at a value smaller than 1%.

The integrals in equations (16) and (17) are evaluated with the help of the normalisation integral,

$$\int_0^a J_0^2(\lambda\rho)\rho d\rho = \left(\frac{a^2}{2}\right)[J_1(a\lambda)]^2 \qquad (20)$$

and the expression,

$$\int J_0(\lambda\rho)d\rho = \left(\frac{\rho}{\lambda}\right)J_1(\lambda\rho) + C \qquad (21)$$

The exactness in the calculation of θ_L and θ_s for the program that was developed according to equations (11) and (12), is of the order of 1%; this percentage could be reduced even more with the inconvenience of a longer computation time.

The numerical solution of equations (14) and (15) was realised according to the Newtonian method and with a precision of the order of 0.1%.

The geometric profile of the interface was obtained by trial and error in the following way:

For each value of ρ in the interval $0 < \rho < 1$, we initially assume that the interface is at $x = 0$; that value is substituted into equation (11) to find a value θ_S; if $\theta_S < \theta_{lq}$, we modify the initial assumption, that is we let $h_{i+1} = h_i + \delta h$; then we calculate a new value of θ_S and the process is repeated until we have $\theta_S = \theta_{sq}$ and the value of h satisfying this relation corresponds to the position of a point of the interface. In the program developed it was fixed $\delta h = 1 \times 10^{-6}$ cm.

A diagram which illustrates the calculation process of h is shown in figure 2.

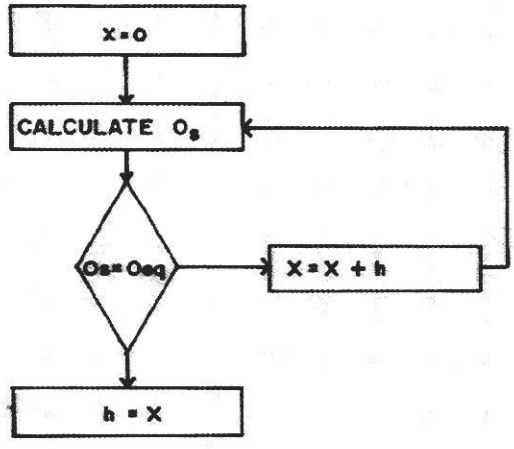

Figure 2 Flow diagram with the logic sequence in order to obtain the interface geometric profile

A general diagram of the program to carry out the numerical solution of the problem for a prefixed value of ρ is the one shown in figure 3.

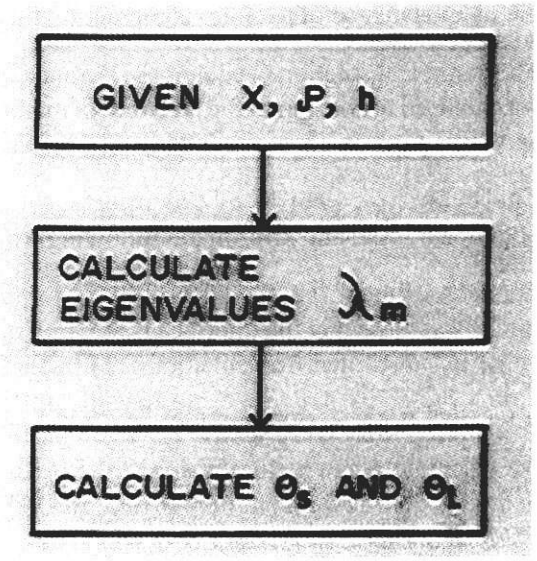

Figure 3 Flow diagram with necessary operations to obtain thermal profiles

The foregoing procedure is repeated for each value of ρ in the interval [0,1] and this allows one to obtain the thermal profiles in the ampoule during the solidification process of the single crystal.

Results

Thermophysical properties of semiconductor $Pb_{1-x}Sn_xTe$ with $x = 0,2$ were used to apply the mathematical model. The steady-state axial and radial temperature profiles of figures 4 to 6 for the solid and liquid phases were obtained. Also, the geometric profile of the interface and its variation is shown as a function of the Biot number and the lowering velocity of the ampoule (figures 7 and 8).

The parameters and coefficients used to generate these profiles are given in table 1.

To construct each of the plots and make its analysis easy, we introduce a dimensionless temperature calculated with respect to T_C:

$$\theta_L^{\backslash} = 1 - \theta_L = \frac{T_L + T_C}{T_H - T_C} \qquad (22)$$

Analysis of the axial termal profiles

Figure 4 shows the axial temperature profiles for two different velocities of the motion of the ampoule, keeping the remaining variables constant, which is equivalent to changing the Peclet number. For axial distances in the interval $0 < x < 24$ it holds that for each value of x, the number Pe decreases with an increase in temperature θ; this fact is present only in the solid phase.

Also, from figure 4 we notice that the axial temperature gradient, given by the slope of the curve ($d\theta/dx$), increases smoothly from a value that is almost vanishing at $x = 0$ until it reaches a maximum value in the neighborhood of the interface [7-8].

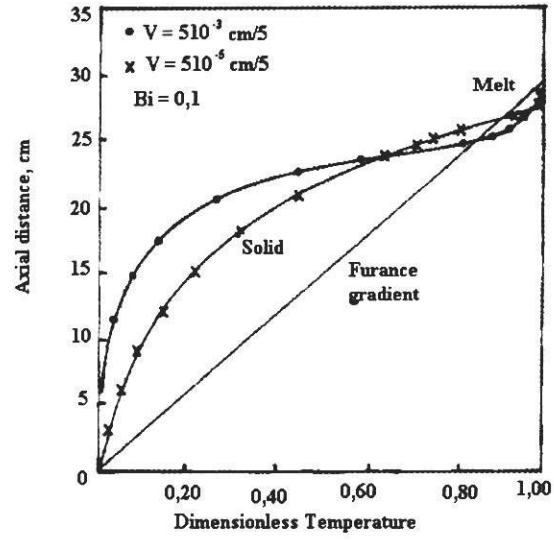

Figure 4 Axial temperature profile as a function of the lowering velocity of ampoule and for Bi = 0,1

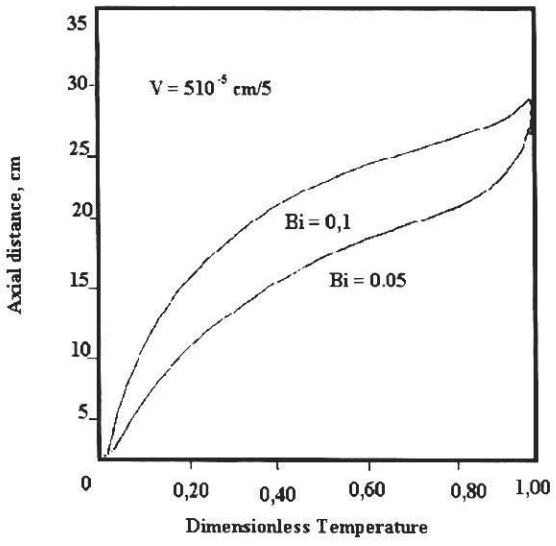

Figure 5 Axial temperature profile as a function of the Biot number for a lowering velocity v=5 x 10^{-5} cm/s

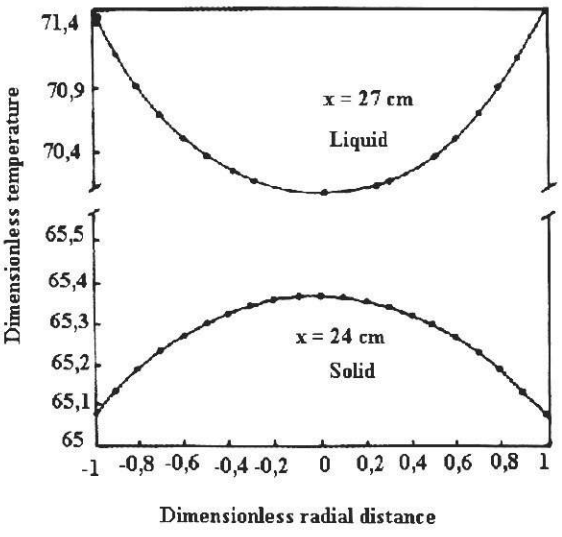

Figure 6 Radial thermal profile both for solid and liquid phases for a Biot number Bi = 0,1 and a lowering velocity v = 5x10^{-5} cm/s. Concave and convex shapes are respectively observed in the solid and liquid phases

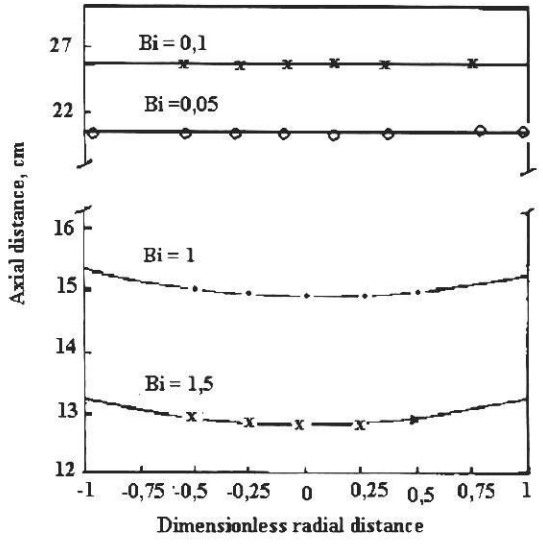

Figure 7 Influence of the Biot number on the morphology of the interface for a velocity v = 10^{-5} cm/s

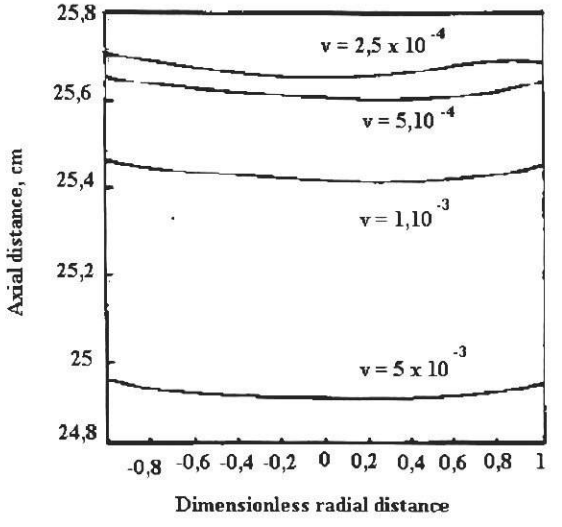

Figure 8 Influence of the lowering velocity of the ampoule for a Biot number of 0,1. It is observed that for velocities higher then 10^{-5} cm/s the interface is not plane, such as it was notice from figure 7

The term $\left(\frac{V}{\alpha}\right)\left(\frac{\partial T}{\partial x}\right)$ in equation (1), represents the rate of change of the internal energy of the solution per unit volume and it can be stated that such an energy increases proportionally to the axial distance, until a maximum in the neighborhood of the interface.

For values $x > 24$, which correspond to the liquid phase, the behaviour is reversed and an increase of both temperature and the Peclet number is noticed. This is in agreement with the fact of the lowering velocity of the ampoule increases, both the rate of cooling and decreasing of the internal energy are increased.

For the liquid phase the behaviour is opposite to the one described above, due to the fact that its properties are different from those of the solid and mainly due to its larger thermal diffusivity.

Likewise, it can be verified that the maximum temperature difference between the two curves of figure 4 in the liquid phase represents 42% of the maximum temperature difference recorded in the solid phase.

An additional factor which contributes to decrease temperature with an increasing velocity of the ampoule is segregation, but this phenomenon has not been considered in this model [9-12].

Influence of the Biot number on the thermal profiles

The influence of the Biot number on the axial temperature profile, keeping the lowering velocity of the ampoule constant, is shown in figure 5. The two values of *Bi* indicated there correspond to the solid phase; for the liquid phase. The value of *Bi* is proportional to Bi_s and is given by

$$Bi_L = \frac{K_S}{K_L} Bi_S \qquad (23)$$

Figure 5 suggests that at each point along the ampoule temperature increases when the value of *Bi* decreases. The same happens with the value of the slope $\frac{\partial \theta}{\partial x}$

The Biot number *Bi* can be interpreted as the ratio of the heat transfer at the surface of the ampoule to the heat conduction in the semiconductor material, or, in other words, the ratio of the internal thermal resistance (a / k_i) of the sample to the external thermal resistance $(1/H)$ of the furnace [9, 13].

As in this case the thermal conductivity K_i and the radius a of the ampoule have been kept constant, the decrease in the value of *Bi* is due to the decrease in the heat transfer coefficient (H) of the furnace, which depends on the characteristic thermal configuration or on design parameters of the furnace [9, 14].

On the basis of the foregoing, from figure 5 we can infer that upon decreasing the heat transfer at the surface of the ampoule, temperature increases at each point.

When the Biot number is small ($Bi < 0{,}1$), as in our case, and when the temperature of the furnace does not change rapidly, a one-dimensional model holds for the heat transfer, which is expressed by:

$$\rho_i Cp_i V \frac{\partial T_i}{\partial x} = -\frac{2H}{a}(T_i - T_\infty) \qquad (24)$$

$i = S, L$ *(solid or liquid)*. In this equation *Cp* is the constant pressure heat capacity, H is the global heat transfer coefficient between furnace and ampoule, ρ_i is sample density; T_i the sample temperature at phase i and T_∞ the interior wall furnace temperature.

The second term on the right corresponds to the heat transfer on the surface of the ampoule and the first term is associated with the axial heat conduction.

Analysis of the radial thermal profiles

The increase in the velocity v is translated into a temperature decrease at each point along the diameter of the ampoule. Furthermore, we can notice that the variation in temperature along the diameter of the ampoule is minimum such as it is seen in figure 6.

For the solid phase the maximum variation in temperature is 0,5% with respect to the lowest temperature that is recorded at the diameter ends.

The small deviation of the radial thermal profile with respect to a completely horizontal and uniform profile, is due to the value of the thermal conductivity of the sample.

The heat conduction in the radial direction is expressed by Fourier's law.

$$q_r'' = -K\frac{\partial T}{\partial r} \qquad (25)$$

Figure 6 shows that the slope of the radial thermal profile ($\frac{\partial T}{\partial r}$) is positive in the interval $-1 < \rho < 0$ and, also, such a profile presents radial symmetry; all of this indicates that heat flows out from the center of the ampoule. The internal conductive resistance of the sample causes the temperature to be maximum at $\rho = 0$ and decrease as ρ increases.

The radial thermal profile in the liquid phase has a concavity opposite to that of the profile for the solid, which means that the radial heat flow in the liquid phase is established from the wall of the ampoule to the inner part of the sample where there is a smaller temperature.

All the results given above satisfy the second law of Thermodynamics, since in both phases the radial heat flow is established between regions of high and low temperatures.

Influence of the lowering velocity and the Biot number on the position and the geometric profile of the interface

The variation of the geometric profile of the interface as a function of velocity v and for $Bi = 0,1$ is shown in figure 8, while the influence of the Biot number on the shape of the interface for $V = 5 \times 10^{-5}$ cm/s can be seen in figure 7.

A convex morphology will favour the grain selection, that is, a preferential growth direction; and a plane one will decrease thermal stresses which may generate defects such as dislocations , point vacancies, etc. Consequently, a flat morphology is desirable.

In figure 8 we also notice that the shape of the interface is likewise linked to its axial position. This is explained if we take into account that the shape of the interface depends on the ratio of the axial thermal gradient (dT/dx) of the solution to the lowering velocity V [5, 14] and on the thermal gradient of the furnace.

The transition from a plane interface to another more curved one and bearing a less regular structure is related to a smaller value of the relation $((dT/dx)/V)$. This gradient is strongly influenced by the thermal profile of the furnace (the straight line in figure 4).

The location of the interface depends on all the parameters that describe thermal profiles such as the Biot number, the Peclet number, the latent fusion heat, the temperature difference $T_H - T_C$, the lowering velocity of the ampoule, etc.

Figure 9 corresponds to $Bi = 0,1$ and there we can observe that for small values of the velocity ($V < 0,001$ cm/s) and, therefore, of the Peclet number, the position of the interface changes considerably. Also, in this figure we can notice that as the lowering velocity of the ampoule increases, the axial position of the interface descends as a consequence of the temperature decrease, due to an increase in the solidification

velocity, of the heat transported by the ampoule, of the latent heat release at the interface, of the difference between the thermal properties of the solid and liquid phases and of the melting flow on free convection of the melting flow.

In all the velocity range analysed above, the position of the interface descends with an increasing velocity. It is possible that while the larger the lowering velocity is there is a decrease in the sensible heat transfer associated with the overheated melting and in the latent fusion heat which must move through the interface, the solid formed and the ampoule. This would cause a decrease in the proportion of solidified semiconductor and a smaller length of the column of the solid formed.

A small lowering velocity would allow more heat transfer and, therefore, the solid column will be longer.

The influence of Biot number on the location of the interface is abnormal since for a low Biot number *(Bi)*, the interface position is near the furnace hot zone, and for a higher one, the interface axial coordinate *(h)* is near the furnace cold zone.

Influence of the lowering velocity on the steady state

It has been found [1, 2, 7] that the transient behaviour causes a difference between the growth velocity of the crystal $R(t)$ and the translation velocity of the ampoule. Such a difference becomes evident when sudden changes in the velocity of the ampoule are present and it influences both axial and radial heat transfers; it also influences latent heat release at the interface and the growth of the crystal.

Furthermore, it must be kept into account that for low advance velocities of the ampoule, the solidification front tends to be plane, because this is the minimum energy configuration. Upon increasing the lowering velocity, a deviation with respect to equilibrium conditions appears and the interface may become a curve or acquire a dendritic structure unfavourable for the formation of the single crystal.

Increasing the lowering velocity is equivalent to increasing the rate of decrease of the internal energy and the rate of cooling, which causes the solidification front to become unsteady and the interface to cease to be plane.

Conclusions

A mathematical two-dimensional model was developed to describe the heat transfer for the steady state furnace operation, during the one-directional solidification of the single crystal in Bridgman-Stockbarger furnaces.

With this model it was possible to obtain axial and radial thermal profiles for the liquid and solid phases of the growth and to analyse the influence that the Biot number and the lowering velocity of the ampoule have on these profiles.

The results obtained allowed to analyse the behaviour of the internal energy both in the melting and in the solid, the same as the influence of the thermal properties of the grown material on the profiles obtained.

It was gained to establish that an increase in the lowering velocity of the ampoule causes a temperature decrease in the liquid phase and a dissension in the axial position of the interface.

An increase in temperature for the liquid phase can be gained by decreasing the Biot number, which brings the additional consequence that the interface moves downwards.

The radial thermal profiles furnish valuable information about heat flow on the surface of the ampoule and about the influence of the Biot number during solidification.

It was determined that the shape and position of the interface depend on a complex interdependence of all the parameters that have influence on the thermal profiles such as the Biot

and Peclet numbers, the temperature gradient and the lowering velocity of the ampoule.

Acknowledgements

The authors gratefully acknowledge Colciencias for sponsored the presentation of this paper in "Physics Meeting 94" in Cancun, Mexico.

References

1. Bourret E. D., Brown R. A. and Derby J. J.: *Journal of Crystal Growth*. 1985, 71. pp. 587-596.
2. Duffar T. and Barat C. *Materials Science & Enginnering*. 1993. A173. pp. 15-18.
3. Steer C.H., Hage-Ali M. and Siffert P.: *Materials reserach Society Symposium Proceedings*. 1993, 302. pp. 237-242.
4. Viskanta R. *Journal of Heat Transfer*. 1988, 110. pp. 1.205-1.219.
5. Davey K. *Applied mathematical* Modelling. 1993, 17. pp. 658-663.
6. Mahmoud K. G. *Computers & Chenical* Engineering. 1993, 17. pp. 705-715.
7. Chidiac S. E. and Brimacombe J.K. *Applied scientific research*. 1993, 15. pp. 573-597 (1993).
8. Lin CH. and Motakef S. *Journal of Crystal Growth*. 1993, 18. pp. 834-841.
9. Banan M., Gray R. and Wilcox W. *Journal of crystal growth*. 1991, 113. pp. 557-565.
10. Tien R. H. *Trans. of the ASME*. 1972, 50. pp. 65-70.
11. Heurtault S., Badie J. M. and Rouanet A. *Journal of Heat Mass Transfer*. 1982, 25. pp. 1.671-1.676.
12. Guzmán J. A. *Apuntes de ingeniería*. 1981, 4. pp. 19-34.
13. Incropera F. and Dewith D. P. *Fundamentals of heat Transfer*. 4th ed. New York. John Wiley & sons.
14. Hejne F., Agimova T. and Cortés M. *Revista de Ciencia de la Universidad del Valle*. 1993. 8.